High-spin collective structures in ^{178}Pt

F. G. Kondev, M. P. Carpenter, R. V. F. Janssens, I. Wiedenhöver, M. Alcorta, L. T. Brown,* C. N. Davids, T. L. Khoo, T. Lauritsen, C. J. Lister, D. Seweryniak,† S. Siem,‡ A. A. Sonzogni, and J. Uusitalo§
Physics Division, Argonne National Laboratory, Argonne, Illinois 60439

P. Bhattacharyya
Department of Chemistry, Purdue University, West Lafayette, Indiana 47907

S. M. Fischer
Department of Physics, DePaul University, Chicago, Illinois 60614

W. Reviol and L. L. Riedinger
Department of Physics and Astronomy, University of Tennessee, Knoxville, Tennessee 37996

R. Nouicer
Department of Physics, University of Illinois at Chicago, Chicago, Illinois 60607
(Received 12 November 1999; published 20 March 2000)

Collective structures in ^{178}Pt have been investigated with γ-ray spectroscopic techniques following mass selection. The present data expand considerably the level scheme of this nucleus. A new collective structure has been identified and the known bands have been extended to higher spins. Firm spin and parity assignments have been made to many levels. Of particular interest are the negative parity bands which are interpreted in terms of structures associated with octupole vibrations crossed at moderate spin by two-quasiparticle excitations. The systematics of the α-decay reduced widths in Pt nuclei has also been investigated. The differences of a factor of about 2 between the widths for the odd- and the even-A isotopes is attributed to changes in neutron pairing associated with the blocking effect. The trend is reproduced in calculations based on the Lipkin-Nogami pairing model.

PACS number(s): 21.10.Re, 23.20.Lv, 27.70.+q, 21.10.Tg

I. INTRODUCTION

Despite their close proximity to the $Z=82$ shell closure, the Pt ($Z=78$) nuclei of the $A\sim180$ region are characterized by level structures associated with prolate, oblate, and triaxial deformations. In these nuclei, excitations based on the intruder orbitals have received considerable attention because of their ability to affect the nuclear shape. In particular, it has been shown that the prolate minimum is associated with multi-particle-hole excitations across the $Z=82$ shell gap involving the $h_{9/2}$, $f_{7/2}$, and $i_{13/2}$ proton intruder orbitals [1,2]. While in the Os ($Z=76$) nuclei the quadrupole deformation is approximately constant over a wide range of isotopes, there is evidence in the Hg ($Z=80$) isotopes that structures built upon specific intruder orbitals impact the nuclear shape significantly. Specifically, Ma *et al.* [3] have shown in ^{186}Hg that the occupation of the $1/2^+[651]$ ($g_{9/2}$) and $1/2^-[770]$ ($j_{15/2}$) neutron orbitals drives the nucleus towards a prolate deformation value of $\beta_2\sim0.35$ which is intermediate between those associated with the normally deformed ($\beta_2\sim0.25$) [3] and the superdeformed ($\beta_2\sim0.50$) [4] minima. It has been shown recently that proton excitations involving the $1/2^+[660]$ ($i_{13/2}$) and $1/2^-[541](h_{9/2})$ orbitals also have a shape driving effect on collective structures in ^{178}Hg [5] and ^{180}Hg [6]. Furthermore, mean-field calculations by Nazarewicz [7] with a Woods-Saxon potential predict that, for neutron number $N<98$, the prolate minimum evolves from $\beta_2\sim0.25$ towards larger deformations of $\beta_2\sim0.50$–0.56, but the excitation energy for this minimum rises to approximately 3.5 MeV. In addition to the shape coexistence phenomena, nuclei in this region also exhibit a variety of other collective and quasiparticle excitations. For example, excited negative parity bands, consisting of cascades of stretched quadrupole transitions, have been discovered near the yrast line of many even-even Os, Pt, and Hg nuclei [3,5,6,8–16]. At low spin their configurations are usually associated with an octupole vibration [5,6,8,9,11,12,14], although an interpretation in terms of quasiparticle excitations has also been proposed [10,15].

In this general context the study of Pt nuclei is worthwhile as it is likely to add information on the relative importance of various orbitals for the collective excitations in this mass region.

This paper presents new data on the neutron-deficient ^{178}Pt ($N=100$) nucleus obtained as a by-product of an experiment investigating the structure of ^{178}Hg [5]. As one

*Also at: Department of Physics, Vanderbilt University, Nashville, TN 37235.

†Also at: Department of Chemistry, University of Maryland, College Park, MD 20742.

‡Also at: Department of Physics, University of Oslo, N-0316 Oslo, Norway.

§Present address: Department of Physics, University of Jyväskylä, P.O. Box 35, 40351 Jyväskylä, Finland.

TABLE I. α decay properties of the ^{178}Pt ground state.

Nucleus	J_i^π	J_f^π	present			previous [22]			
			E_α (keV)	I_α (%)	$T_{1/2,\alpha}$ (s)	E_α (keV)	I_α (%)	$T_{1/2,\alpha}$ (s)	b_α (%)
^{178}Pt	0^+	0^+	5447(4)	96.5(29)	20(1)	5446(3)	94.9(24)	21.1(6)	7.46(28)[a]
		2^+	5289(8)	3.5(4)		5291(4)	5.1(24)		

[a]The α-decay branch b_α is taken as a weighted average of the values given in Refs. [29,30].

approaches the proton drip line, it becomes increasingly difficult to produce states of high spin and excitation energy in nuclei by using conventional heavy-ion fusion reactions owing to severe competition from fission and charged particle emission. Furthermore, the remaining evaporation-residue cross section is fragmented over many channels, thus requiring sensitive detection techniques to select the nucleus of interest. This was achieved here by using the prompt γ-ray coincidence technique following mass selection, as well as the recoil-decay tagging technique [17].

II. EXPERIMENTAL PROCEDURE AND DATA REDUCTION

A. The experiment

Excited states in ^{178}Pt were populated with the ^{103}Rh(^{78}Kr,3p) reaction using 350-MeV beams provided by the ATLAS superconducting linear accelerator at the Argonne National Laboratory. The experimental method is similar to that described in Ref. [18]. Specifically, the target consisted of a 480 μg/cm^2 self-supporting foil. Prompt γ rays were detected with the Gammasphere array [19], consisting, for this experiment, of 101 large volume escape-suppressed Ge detectors arranged in 16 rings located at angles $\theta = 31.7°$, $37.4°$, $50.1°$, $58.3°$, $69.8°$, $79.2°$, $80.7°$, $90.0°$, $99.3°$, $100.8°$, $110.2°$, $121.7°$, $129.9°$, $142.6°$, $148.3°$, and $162.7°$ relative to the beam direction. The recoiling products were passed through the Argonne fragment mass analyzer (FMA) [20] and were dispersed according to their mass-to-charge (m/q) ratio. A position-sensitive parallel grid avalance counter (PGAC), located at the focal plane, provided the m/q information as well as time of arrival and energy-loss signals of the evaporation residues. The recoiling nuclei were subsequently implanted into a 40×40 strips (40 mm$\times$40 mm, $\sim$60 μm thick), double-sided silicon strip detector (DSSD) located 40 cm behind the PGAC. The DSSD events were also time-stamped using a 48-bit, 1 MHz latching clock. An efficient time correlation was achieved between implanted recoils, subsequent α decays and the preceding prompt γ-ray flash.

B. Data reduction

To isolate the ^{178}Pt residues and the corresponding prompt γ rays from the dominating background contributions originating from scattered beam, fission products and deexcitations in neighboring isotopes, coincidence gates were placed in the off-line analysis on (i) the time of flight of the evaporation residues from the target to the focal plane, (ii) the PGAC positions corresponding to three charge states ($q = 31$, 32, and 33) of ions with the appropriate $A = 178$ mass focus (iii) the two-dimensional histogram of the energy of recoils measured in the DSSD vs the time of flight from the PGAC to the DSSD. These conditions were applied in every sorting of the data. A total of 1.4×10^8 coincidence events were written to tape either when two or more Gammasphere detectors fired in coincidence with the PGAC and/or DSSD counters, or when a charged-particle decay was detected in the DSSD. About 2.7×10^6 of these events included correlations between γ rays detected at the target position and fusion-evaporation residues measured in the PGAC (recoil-γ events), and approximately 9.3×10^5 events included an additional correlation within a pixel of the DSSD between an implanted residue and its subsequent α decay (implant-α-decay events). Approximately 60% of all the mass selected events were associated with ^{178}Pt.

1. Recoil-γ-γ and recoil-γ-γ-γ events

The γ-ray data were sorted into E_γ-E_γ and E_γ-E_γ-E_γ histograms of coincidence events occurring within a 100 ns time window. Since the γ-ray emission occurs when the recoiling nuclei are in flight ($v/c \sim 4\%$), the γ-ray energies were corrected for the Doppler shift. To reduce the interference from Coulomb excitation (random coincidences) only events where more than four detectors fired in prompt coincidence were used in the construction of histograms. Background subtracted spectra were then produced for each particular cascade and were examined with the RADWARE [21] interactive software package in order to construct the level scheme. To enhance the ^{178}Pt γ rays from those produced by other $A = 178$ residues, an additional γ-γ coincidence matrix gated by the characteristic ^{178}Pt α line of $E_\alpha = 5446$ keV [22] was created. Due to the weak α branch (see Table I), the statistics of the resulting γ-ray spectra were not sufficient to obtain reliable coincidence information. Nevertheless, most of the γ rays assigned to ^{178}Pt were identified in the total projection of this matrix, hereby confirming the isotopic assignment.

2. γ-ray angular distributions and anisotropies

Angular distributions were obtained by projecting spectra corresponding to γ rays detected in a specific ring of detectors in Gammasphere. From these spectra the intensities of the strongest γ rays were measured and then fitted with the usual expression

$$W(\theta) = 1 + A_2 P_2(\cos\theta) + A_4 P_4(\cos\theta), \qquad (1)$$

where A_2 and A_4 are the angular distribution coefficients (the normalization factor A_0 has been omitted for simplicity) and

$P_l(\cos\theta)$ are the Legendre polynomial functions. The limited angular distribution information was extended further by extracting the anisotropy ratio R defined as the intensity ratio of transitions observed at the 31.7° (and the equivalent 148.3°) and 37.4° (142.6°) detector rings to those detected at the 79.2° (100.8°), 80.7° (99.3°), and 90.0° rings of detectors. In general, values greater than unity indicate a stretched quadrupole or mixed $M1/E2$, $\Delta J=1$ transition with a positive sign for the mixing ratio, δ. Values of $R<1$ are associated with a pure dipole or mixed $M1/E2$, $\Delta J=1$ transition with $\delta<0$. These assignments were checked with a number of transitions of known multipolarity in the neighboring ^{177}Pt nucleus [23], populated via the $3pn$ channel in the present experiment. For example, $R=0.34(6)$ and 1.20(4) values were deduced for the 176.2 and 473.0 keV γ rays in ^{177}Pt, which were reported in Ref. [23] to have mixed $M1/E2$ [$A_2=-0.54(11)$] and $E2$ [$A_2=0.18(5)$] multipolarities, respectively.

3. Recoil-$E_\alpha-\Delta t_\alpha$ events

A two dimentional histogram with the energies of the first generation α decays E_α on one axis and the difference between the implantation and α-decay times Δt_α on the other was constructed after matching the individual energy signals of all DSSD strips. Energy spectra gated on different regions of the time axis were then constructed and used to deduce the α-decay energies and intensities. The selection of specific time regions significantly reduced the complexity of the α-energy spectra as well as the background due to random coincidence events. Time spectra were generated for each α line and used to determine the half-life of the emitting state, using the least-square fitting method [24].

III. EXPERIMENTAL RESULTS

A. Previous studies

The α decay of the ^{178}Pt ground state has been studied previously by several authors (see for example Ref. [22], and references therein). The $J^\pi=2^+$ state at 170 keV as well as the excited 0^+ state at 422 keV (not observed in the present data) were populated in the α decay of ^{182}Hg [25,26]. The β^+/(EC)-decay work of Davidson *et al.* [27] extended the ^{178}Pt level scheme up to a moderate spin of $9\hbar$. Using the ^{144}Sm(^{37}Cl,$p2n$) reaction, Dracoulis *et al.* [28] reported the first in-beam measurements. These authors identified the ground state band up to 18^+ and measured the level lifetimes in this band up to 8^+, excluding the 2^+ state. Recently, Soramel *et al.* [13] confirmed the observations of Ref. [28] by using the ^{142}Nd(^{46}Ti,$2\alpha2n$) reaction. In addition, they reported a new band which was tentatively assigned odd spins and negative parity.

B. α-decay measurements

Figure 1(a) presents an α-energy spectrum correlated with $A=178$ residues within the time interval of 20 to 60 s following an implantation into the same DSSD pixel. As summarized in Table I, the data confirm the previously reported

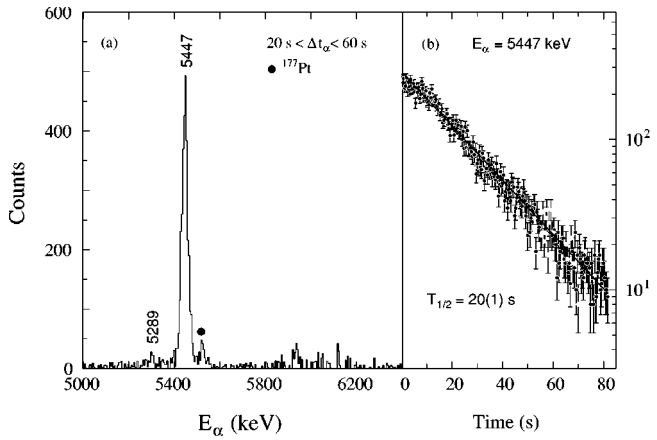

FIG. 1. (a) α energy spectrum measured within the time interval of 20 up to 60 s after the implantation of a recoil with $A=178$ in the DSSD. (b) Time spectrum produced by gating on the $E_\alpha=5447$ keV line.

lines connecting the ^{178}Pt ground state with the 0^+ and 2^+ levels of the ^{174}Os daughter nucleus. Using the time spectrum produced by gating on the 5447 keV line [Fig. 1(b)], a half-life of 20(1) s was obtained for the ^{178}Pt ground state, in agreement with values reported previously [22]. However, due to the limited statistics, it was not possible to obtain reliable lifetime information for the 5289 keV line.

C. Level scheme construction

The level scheme of ^{178}Pt deduced from the present study is shown in Fig. 2. The assignment of γ rays is based on the observed correlation with the characteristic $E_\alpha=5447$ keV line and on measured coincidence relationships with previously known transitions in ^{178}Pt [13,28], and with the characteristic Pt x rays. The γ rays assigned to ^{178}Pt are listed in Table II together with their intensities, angular distribution and anisotropy coefficients, and proposed multipolarities. Some relative γ-ray intensities were obtained from the total projection of the recoil-γ-γ matrix, others were extracted from coincidence projections after appropriate normalization. Although angular correlations could affect the measured intensities (at a ~10% level), no corrections were applied.

The spin and parity assignments are based mainly on the angular distribution and anisotropy information. The present measurements were not sensitive to the identification of isomeric states because the residues fly out of the focus of Gammasphere into the FMA. Hence, only $E1$, $M1$, and $E2$ multipolarities were considered. In addition, γ-ray intensity balances were used to deduce the total internal-conversion coefficients α_T for transitions with energy below about 200 keV. In this way it was possible to distinguish between $E1$, $M1$, and $E2$ transitions. Several of the assignments are tentative. These are indicated under parenthesis in Fig. 2 and in Table II. Furthermore, additional arguments such as the relative population of levels within a given band, the absence of certain transitions and the band structure itself have been used to remove possible ambiguities.

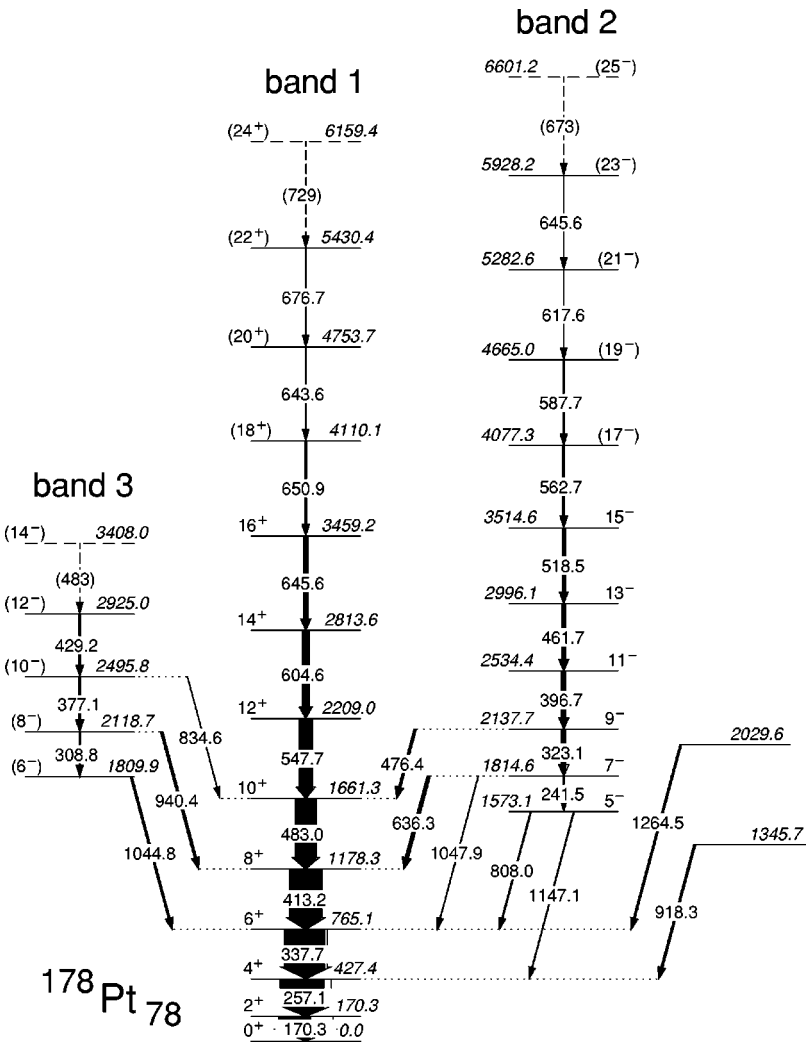

FIG. 2. Level scheme of ^{178}Pt deduced from this work. Tentative placements are indicated by dashed lines. Tentative spin-parity assignments are given in brackets.

1. Band 1

A sample spectrum showing the γ rays in coincidence with the 483.0, 547.7, 604.6, 645.6, and 650.9 keV transitions above the 8^+ level of the ground state band is presented in Fig. 3(a). Compared to previous work [13,28], this band is extended in spin up to 22^+ (tentatively 24^+). The angular distribution and anisotropy information is consistent with a stretched quadrupole character for all in-band γ rays up to the 16^+ state. In addition, the intensity balance at the 2^+ level yields $\alpha_T = 0.65(5)$ for the 170.3 keV transition. This can be compared with expected values of 0.67 for $E2$, 1.65 for $M1$, and 0.11 for $E1$ multipolarities [31]. It should be noted that in the level scheme of Ref. [13], the $10^+ \rightarrow 8^+$ in-band transition is labeled as 428 keV, compared to values of 483.0 and 482.0 keV reported in the current work and in that of Ref. [28], respectively.

2. Band 2

A coincidence spectrum showing γ rays associated with band 2 is presented in Fig. 3(b). Compared to the work of Soramel *et al.* [13], this sequence is extended in spin up to 23^- (tentatively 25^-). It is worth noting that the 562.7(3) keV energy of the $17^- \rightarrow 15^-$ in-band transition differs from that given in Ref. [13] as 570.0(5) keV. Three new interband transitions of 476.4, 1047.9, and 1147.1 keV have also been added (Fig. 2). The states at 1573.1, 1814.6, and 2137.7 keV were also reported by Davidson *et al.* [27], but the 241.5, 476.4, and 1047.9 keV transitions were not placed in their level scheme.

This band is assigned odd spins and negative parity on the basis of a number of arguments. The angular distribution coefficients for the 636.3 keV γ ray (Table II) support a dipole character and are incompatible with a $J \rightarrow J$ possibility for the full range of the quadrupole/dipole mixing ratio [32]. A possible $J \rightarrow J$-1 assignment, leading to $9^-(9^+)$ for the 1814.6 keV level, would imply that the 1047.9 keV γ ray, which connects this state with the 6^+ level of the ground state band, has an $E3$ ($M3$) multipolarity. Given the measured branching ratios for decays from the 1814.6 keV level (Table I) and the Weisskopf partial lifetime estimate for the 1047.9 keV γ ray, one would then expect a half-life of about 60 ns (~ 6 μs) for this level, which contradicts the present observations. Thus, the 636.3 keV γ ray must correspond to a $J \rightarrow J+1$ transition and, hence, $J=7$ is assigned to the 1814.6 keV state. A negative parity is favored given the measured branching ratios for the 1573.1 and 1814.6 keV

TABLE II. Excitation energies, spins, parities, γ-ray energies, intensities, angular distribution coefficients and anisotropies for structures assigned to ^{178}Pt.

E_x (keV)	J_i^π ($\hbar$)	E_γ (keV)[a]	I_γ (rel.)[b]	A_2/A_0	A_4/A_0	R[c]	Assignment
Band 1							
170.3	2^+	170.3	730(30)	0.20(4)	0.08(5)	1.2(1)	$E2$
427.4	4^+	257.1	1000(40)	0.12(4)	-0.03(5)	1.2(1)	$E2$
765.1	6^+	337.7	915(52)	0.12(6)	0.03(7)	1.1(1)	$E2$
1178.3	8^+	413.2	709(64)	0.36(5)	0.13(5)	1.4(1)	$E2$
1661.3	10^+	483.0	471(35)	0.28(6)	-0.09(7)	1.3(1)	$E2$
2209.0	12^+	547.7	300(30)	0.30(6)	0.02(7)	1.4(1)	$E2$
2813.6	14^+	604.6	161(25)	0.23(11)	-0.12(12)	1.2(2)	$E2$
3459.2	16^+	645.6	107(20)	0.24(8)	0.04(10)	1.1(2)	$E2$
4110.1	(18^+)	650.9	40(6)				$(E2)$
4753.7	(20^+)	643.6	<10				$(E2)$
5430.4	(22^+)	676.7	<10				$(E2)$
6159.4	(22^+)	(729)	<10				$(E2)$
Band 2							
1573.1	5^-	808.0	24(4)				$(E1)$
		1147.1	18(3)				$(E1)$
1814.6	7^-	636.3	75(7)	-0.17(9)	0.07(12)	0.6(1)	$E1$
		241.5	20(4)			1.2(2)	$E2$
		1047.9	14(3)				$(E1)$
2137.7	9^-	476.4	53(9)				$(E1)$
		323.1	98(13)	0.21(12)	-0.03(14)	1.3(1)	$E2$
2534.4	11^-	396.7[d]	101(12)	0.16(4)	-0.06(6)	1.2(2)	$E2$
2996.1	13^-	461.7	92(20)	0.30(11)	-0.10(12)	1.4(2)	$E2$
3514.6	15^-	518.5	69(16)			1.4(2)	$E2$
4077.3	(17^-)	562.7	40(8)				$(E2)$
4665.0	(19^-)	587.7	23(5)			1.4(3)	$E2$
5282.6	(21^-)	617.6	<10				$(E2)$
5928.2	(23^-)	645.6	<10				$(E2)$
6601.2	(25^-)	(673)	<10				$(E2)$
Band 3							
1809.9	(6^-)	1044.8	43(8)				$(E1)$
2118.7	(8^-)	940.4	51(7)				$(E1)$
		308.8	24(4)			1.1(2)	$E2$
2495.8	(10^-)	377.1	48(7)			1.3(2)	$E2$
		834.6	10(4)				$(E2)$
2925.0	(12^-)	429.2	40(8)			1.3(2)	$E2$
3408.0	(14^-)	(483)	<10				$(E2)$
other levels							
1345.7		918.3	42(8)				
2029.6		1264.5	39(9)				

[a]Energies are accurate to within 0.1-0.2 keV for the strong transitions. For other transitions the uncertainty may rise up to 0.8 keV.

[b]Relative intensities deduced from the total projection of the recoil-γ-γ matrix, as well as from coincidence projections after appropriate normalization. (See the text for details.)

[c]Angular anisotropy coefficients. (See the text for details.)

[d]Contaminated with the stronger 396.6 keV line in ^{178}Hg [5].

levels. Indeed, the inter-band $J \rightarrow J+1$ transitions are observed to be strongly favored over the competing $J \rightarrow J-1$ decays, despite the fact that the larger energy difference should favor the latter. This observation can be accounted for if the transitions are of $E1$ character, as will be discussed in detail in Sec. IV A 2, but are harder to understand if a $M1$ character is assumed. Hence, negative parity is assigned to band 2.

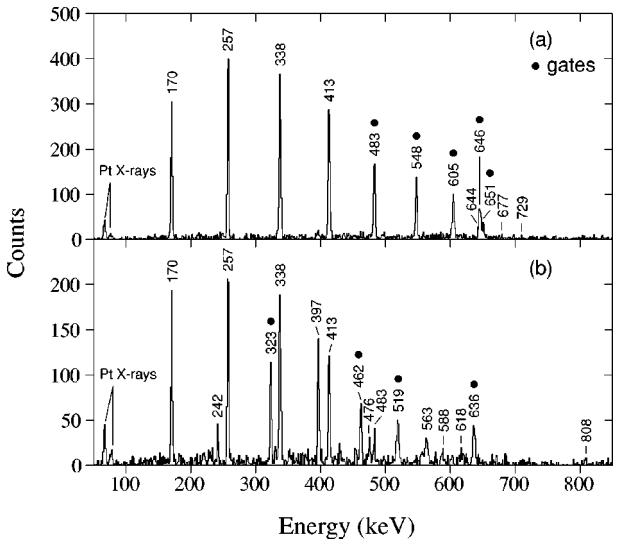

FIG. 3. Summed, background-subtracted γ-ray coincidence spectra from the recoil-γ-γ matrix produced by gating on transitions in band 1 (a) and band 2 (b).

3. Band 3

This band is observed for the first time in the present work, although the 1809.9 keV level and the corresponding 1044.8 keV depopulating transition were reported in Ref. [27]. Spins are assigned tentatively, based on population intensity arguments. For example, the ratio of 0.48(9) between the intensities of the 377.1 keV γ ray (band 3) and the 396.7 keV transition (band 2) would suggest that the spin of the 2495.8 keV level is at least one unit less than that of $11\hbar$ assigned to the 2534.4 keV level. The nonobservation of transitions from the first three in-band levels to the 4^+, 6^+, and 8^+ members of the ground state band (e.g., $6\rightarrow4^+$, $8\rightarrow6^+$, and $10\rightarrow8^+$) favors negative parity for band 3. Also, the proposed assignments are consistent with the systematic features of neighboring even-even Os and Pt isotopes [9,14].

IV. DISCUSSION

A. Structure of the negative parity bands

Negative parity bands have been observed in a number of neighboring even-even Os and Pt isotopes. Their configurations, however, are still the subject of frequent discussions. Dracoulis *et al.* [9] and de Voigt *et al.* [14] interpreted the bands in ^{176,178,180}Os and ^{180}Pt as single-phonon octupole vibrations at low spin crossed by two-quasiparticle excitations at higher angular momentum. A similar interpretation has been invoked by Cederwall *et al.* [12] in their study of ^{176}Pt. On the other hand, Popescu *et al.* [15] and Lieder *et al.* [10] proposed a pure two-quasiparticle assignment for the negative parity structures in ^{182}Pt and ^{180}Os, respectively. In their recent work Soramel *et al.* [13] suggested that the negative parity band in ^{178}Pt, labeled in the present work as band 2, has a decoupled two-quasiparticle $\pi h_{9/2}$ configuration with an admixture of octupole vibrations of unspecified magnitude.

In a deformed nucleus, the structure of vibrational excitations is microscopically viewed as a superposition of a large number of two-quasiparticle excitations. In general, the 3^- octupole phonon splits into states with $K^\pi=0^-$, 1^-, 2^-, and 3^-, each having a well defined rotational band asssociated with it. The bands, however, are usually highly perturbed owing to the strong Coriolis interaction [33]. As shown below, the properties of the negative parity bands in ^{178}Pt, such as the excitation energy of the in-band levels, the strength of the interband $E1$ transitions and the measured alignments, are found to closely resemble those seen in the isotone ^{176}Os [9], where octupole vibrations were invoked at low spin. Hence, this systematic behavior provides additional support for an interpretation of the ^{178}Pt level scheme along the same lines.

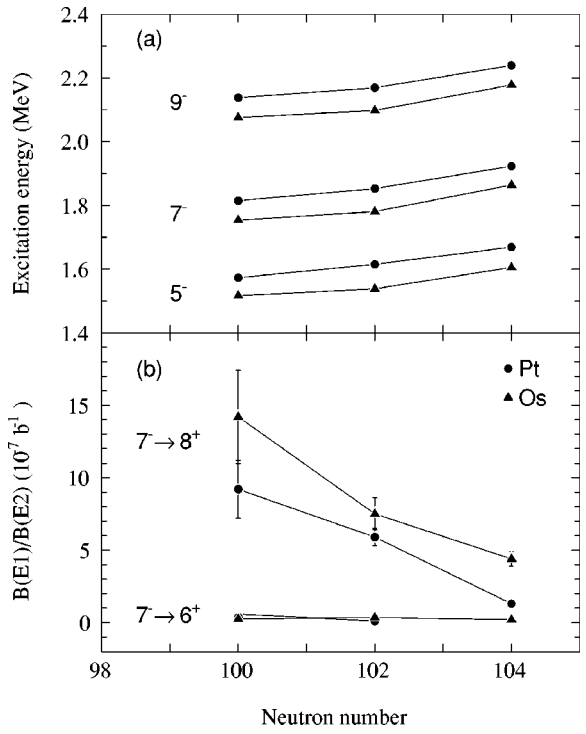

FIG. 4. Excitation energies for the 5^-, 7^-, and 9^- levels (a) and $B(E1)/B(E2)$ ratios for selected transitions (b) in ^{178}Pt and neighboring even-even Os [9] and Pt [14,15] isotopes.

1. Excitation energies

Figure 4(a) presents the excitation energies of the 5^- through 9^- members of the side-bands seen in several even-even Pt and Os nuclei. The small variations with N and Z seen in the figure argue against a pure two-quasiparticle character for these structures, thus supporting their association with octupole vibrations. In order to predict which intrinsic configurations are involved in ^{178}Pt, calculations of the energies of the lowest two-quasiparticle states were carried out using the approach outlined in Ref. [34]. The procedure employs the single-particle energies from the Nilsson model with deformation parameters of $(\varepsilon_2,\varepsilon_4)=(0.233,0.013)$ [35] and the so-called ''standard'' set of potential parameters [36]. The pairing correlations were taken into account within the Lipkin-Nogami formalism, following the prescription of Nazarewicz *et al.* [37], and include the

TABLE III. Calculated excitation energies for low-lying negative-parity, two-quasiparticle configurations in ^{178}Pt.

Configuration[a]		K^{π}_{-}[b]	E^{qp}_{-} (keV)[c]	K^{π}_{+}[b]	E^{qp}_{+} (keV)[c]
π^2	ν^2				
$\Delta j=\Delta l=3\hbar$					
(**1/2**$^-$,**1/2**$^+$)		0^-	2886	1^-	2486
(**1/2**$^{-\prime}$,**1/2**$^+$)		0^-	2784	$\underline{1^-}$	3184
(**1/2**$^-$,3/2$^+$)		$\underline{1^-}$	2337	2^-	2737
(**1/2**$^{-\prime}$,3/2$^+$)		$\underline{1^-}$	3034	2^-	2634
(**3/2**$^-$,3/2$^+$)		0^-	2730	$\underline{3^-}$	3130
(**1/2**$^-$,1/2$^+$)		$\underline{0^-}$	2848	1^-	2448
(**1/2**$^{-\prime}$,1/2$^+$)		0^-	2747	$\underline{1^-}$	3147
(5/2$^+$,9/2$^-$)		$\underline{2^-}$	2691	7^-	3091
	(5/2$^-$,**5/2**$^+$)	$\underline{0^-}$	1799	5^-	2151
	(5/2$^-$,**7/2**$^+$)	$\underline{1^-}$	1574	6^-	1960
	(5/2$^-$,**9/2**$^+$)	$\underline{2^-}$	2820	7^-	3188
others					
(**1/2**$^-$, 5/2$^+$)		2^-	2592	3^-	2192
(**1/2**$^{-\prime}$,5/2$^+$)		$\underline{2^-}$	2343	$\underline{3^-}$	2743
	(7/2$^-$,**7/2**$^+$)	$\underline{0^-}$	2201	7^-	2015
	(7/2$^-$,**5/2**$^+$)	1^-	2268	$\underline{6^-}$	2082
	(7/2$^-$,**9/2**$^+$)	1^-	3740	$\underline{8^-}$	3284
	(1/2$^-$,**7/2**$^+$)	3^-	2063	$\underline{4^-}$	1635
	(1/2$^-$,**5/2**$^+$)	2^-	2031	$\underline{3^-}$	1931

[a]Protons (π): **1/2**$^-$: 1/2$^-$[541]($h_{9/2}$), **3/2**$^-$: 3/2$^-$[532]($h_{9/2}$), **1/2**$^{-\prime}$: 1/2$^-$[530]($f_{7/2}$), 9/2$^-$: 9/2$^-$[514]($h_{11/2}$), 1/2$^+$: 1/2$^+$[400]($s_{1/2}$), 3/2$^+$: 3/2$^+$[402]($d_{3/2}$), **1/2**$^+$: 1/2$^+$[660]($i_{13/2}$); neutrons (ν): 1/2$^-$: 1/2$^-$[521]($p_{3/2}$), 5/2$^-$: 5/2$^-$[512]($f_{7/2}$), 7/2$^-$: 7/2$^-$[514]($h_{9/2}$), **5/2**$^+$: 5/2$^+$[642]($i_{13/2}$), **7/2**$^+$: 7/2$^+$[633] ($i_{13/2}$); **9/2**$^+$: 9/2$^+$[624] ($i_{13/2}$).

[b]$K_{\pm}=|\Omega_{\pi_1(\nu_1)}\pm\Omega_{\pi_2(\nu_2)}|$. The expected energetically favored states are underlined.

[c]Due to the rapid downslope of the $h_{9/2}$, $f_{7/2}$, and $i_{13/2}$ proton orbitals as deformation increases, the excitation energy of configurations which involve these structures are strongly deformation dependent.

effects of blocking. A model space of 3 oscillator shells ($N=4$, 5, and 6) with 64 levels, for both the neutrons (ν) and protons (π), was used with fixed monopole pairing strengths of $G_{\nu}=20.0/A$ MeV and $G_{\pi}=20.8/A$ MeV. In order to avoid some of the pitfalls introduced by the choice of the potential and deformation parameters, the single-particle energies for neutron and proton levels close to the Fermi surfaces were adjusted so that the observed one-quasiparticle band-head energies in ^{177}Pt ($N=99$) [23] and ^{179}Ir ($Z=77$) [38] are reproduced. High-j, $\Omega=1/2$ orbitals are located near the proton Fermi surface in ^{179}Ir. As a result, the excitation energies of the $I=1/2$ levels are not well defined because of the large decoupling parameter for these orbitals and the strong Coriolis interaction. Hence, the single-particle energy for the 1/2$^-$[541]($h_{9/2}$) and 1/2$^-$[530] ($f_{7/2}$) proton orbitals were adjusted according to the particle-rotor model (PRM) predictions of Ref. [38]. A similar approach was used to account for the single-particle energy of the π1/2$^+$[660] ($i_{13/2}$) level. It should be pointed out that, due to the limited available experimental information on one-quasiparticle excitation energies, only a few levels were adjusted. In all other instances, the values given by the Nilsson model were adopted. Furthermore, the one-quasineutron energies were not corrected for the rotational contribution to the band-head energy ($E_{\rm rot}=\hbar^2K/2\mathcal{F}$, where $\mathcal{F}$ is the moment of inertia) and for the Coriolis energy shift. These corrections were also omitted for the predicted energies of the two-quasiparticle states in ^{178}Pt.

For a given two-quasiparticle configuration, the residual nucleon-nucleon interactions give rise to a doublet with $K_{\pm}=|\Omega_{\pi_1(\nu_1)}\pm\Omega_{\pi_2(\nu_2)}|$. According to the Gallagher-Moszkowski coupling rule [39], the triplet state (parallel intrinsic spins) lies higher in energy compared to the singlet state (antiparallel intrinsic spins). The calculated two-quasiparticle excitation energies in ^{178}Pt were subsequently corrected for the effect of orbital-dependent residual nucleon-nucleon interactions, in a way similar to that described in Ref. [40]. The results of the calculations are presented in Table III.

The enhancement of octupole correlations at low spin is generally correlated with the presence of pairs of orbitals with $\Delta j=\Delta l=3\hbar$ near the Fermi surface (see, for example, Ref. [41], and references therein). Several combinations of such orbitals are located near both the proton and neutron Fermi levels in ^{178}Pt. The predicted negative-parity configu-

TABLE IV. Experimental $B(E1J_i \rightarrow J_f)/B(E2J_i \rightarrow J_i-2)$ ratios and $B(E1J_i \rightarrow J_f)$ values.

J_i^π ($\hbar$)	J_f^π ($\hbar$)	$B(E1J_i \rightarrow J_f)/B(E2J_i \rightarrow J_i-2)(10^{-7}b^{-1})$	$B(E1J_i \rightarrow J_f)(10^{-5}$ W.u.)[a]
7^-	8^+	9.2(20)	5.7(14)
	6^+	0.38(11)	0.24(7)
8^-	8^+	5.5(12)	3.5(8)
9^-	10^+	13.6(29)	8.8(21)
10^-	10^+	2.1(9)	1.4(6)

[a]Deduced from the experimental $B(E1)/B(E2)$ ratios and theoretical $B(E2)$ values. (See the text for details.)

rations which involve such structures are given at the beginning of Table III. According to the calculations, the lowest energy negative parity structures will be built upon the $\nu^2(5/2^-[512],7/2^+[633])_{K=1^-}$, and $\nu^2(5/2^-[512],5/2^+[642])_{K=0^-}$ configurations. (Note, that the latter configuration includes the $5/2^+[642]$ ($i_{13/2}$) neutron which is not observed as a one-quasiparticle state in the chain of neighboring odd-mass Pt isotopes and, therefore, the excitation energy for configurations involving this orbital should be regarded as more uncertain.) As can be seen from Table III, there are also many competing $K^\pi=0^-$ and $1^-\pi^2$ configurations which include the intruder $1/2^+[660]$ ($i_{13/2}$), $1/2^-[541]$ ($h_{9/2}$), and $1/2^-[530]$ ($f_{7/2}$) orbitals. Although they are predicted to be located at somewhat higher excitation energy, they can mix with the ν^2 configurations. From these considerations, it should then come as no surprise that octupole correlations play a role in the low-spin, low-energy spectrum of ^{178}Pt and a microscopic description of the octupole phonon would presumably contain combinations of the various two-quasiparticle configurations given in Table III. Furthermore, it should be also added that the structure of the negative parity bands in ^{178}Pt will differ from that proposed for the heavier W and Os nuclei, where higher-K ν^2 $(7/2^-[503],11/2^+[615])_{K=2^-}$, $\nu^2(5/2^-[512],9/2^+[624])_{K=2^-}$, $\pi^2(5/2^+[402],9/2^-[514])_{K=2^-}$, and $\pi^2(5/2^+[402],11/2^-[505])_{K=3^-}$ configurations are expected to dominate [9,33].

2. E1 transition probabilities

The interband $E1$ decays exhibit properties associated with octupole vibrational structures, as detailed in Refs. [9,14], namely, (i) the $J \rightarrow J+1$ transitions are favored over the competing $J \rightarrow J-1$ branches, despite the larger energy for the latter; (ii) the strength of transitions depopulating odd spin states is larger than those depopulating the even-spin levels. The $B(E1)/B(E2)$ ratios derived from the γ-ray branching intensities are presented in Table IV and are also plotted in Fig. 4(b), together with values obtained for neighboring Os [9] and Pt [14,15] isotopes. The absolute $B(E1)$ values, deduced from the experimental $B(E1)/B(E2)$ ratios assuming calculated $B(E2)$ probabilities [42] obtained with a value of $Q_0=6.4(3)e$ b [28] for the quadrupole moment are also given in Table IV. Taking the decays from the 7^- state as an example, the $B(E1)/B(E2)$ ratio for the $J \rightarrow J+1$ transition to the 8^+ member of the ground state band is $9.2(20)\times10^{-7}$ b^{-1} which is similar in strength to that for the equivalent decay in the isotone ^{176}Os [9]. The absolute $B(E1)$ value of $5.7(14)\times10^{-5}$ W.u. is close to the range expected for an allowed $E1$ transition [43], thus suggesting that $K=0$ or 1 components dominate the wave functions of this state. This is in agreement with the predictions given in Sec. IV A 1. The corresponding values for the $J \rightarrow J-1$ branches are significantly suppressed, presumably due to phase differences arising for transitions with $\Delta K=0$ and 1 [9]. The inter-band $E1$ branches from the 8^+ and 10^+ levels are found to be up to six times weaker compared to the $J \rightarrow J+1$ decays from the neighboring odd-spin states. Such an anomaly can be partially attributed to the contribution of only $\Delta K=1$ components in the former transitions. (Note that for the excited $K^\pi=0^-$ band the Clebsh-Gordon coefficients vanish for $\Delta K=0$, $J \rightarrow J$ transitions.)

As can be seen from Fig. 4(b), there is a systematic decrease in the strength of the $E1$ $J \rightarrow J+1$ interband transitions for the heavier Pt and Os isotopes, thus indicating that changes in the structure of the lowest energy configurations have occurred. In fact, as the neutron number increases, the Fermi level shifts towards the $9/2^+[624]$ and $11/2^+[615]$ orbitals, so that the $\nu^2(5/2^-[512],9/2^+[624])_{K=2^-}$, and $\nu^2(5/2^-[512],11/2^+[615])_{K=3^-}$ configurations will be low in energy. Hence, there will be significant $K=2$ and 3 admixtures in the wave function of the negative parity levels which do not contribute to the allowed dipole decay.

3. Alignments

Figure 5 presents the alignment, i, as a function of the rotational frequency $\hbar\omega$ for structures in ^{178}Pt and ^{176}Os [9]. At low frequencies, the agreement between the two isotones is remarkable, confirming the similarity in the associated configurations. In both nuclei, the ground state band exhibits a crossing around $\hbar\omega \sim 0.32$ MeV with a gain in alignment of $\sim 5\hbar$. In this mass region, this can be attributed to the alignment of a pair of $i_{13/2}$ neutrons [44]. The alignment gains at low frequency of approximately $2\hbar$ for bands 2 and 3 are consistent with the contributions expected from an octupole phonon. Band 2 begins to upbend at $\hbar\omega \sim 0.28$ MeV, i.e., at a somewhat lower frequency than seen in the band 1. As suggested by Vogel [45], this behavior can be understood as a crossing of the octupole band with an excited two-quasiparticle structure. A similar interpretation has been invoked for the neighboring Os [9] and Hg [5,6] nuclei, where analogous crossings have been reported. The issue then is the structure of the two-quasiparticle band. As

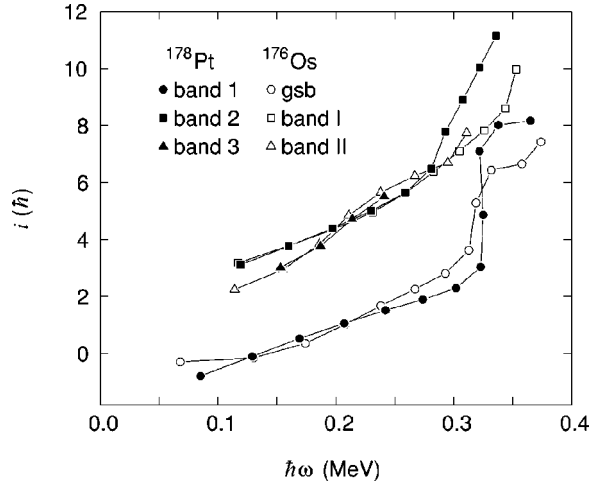

FIG. 5. Aligned angular momenta for the bands in ^{178}Pt (filed symbols) and ^{176}Os (open symbols) [9]. Reference parameters of $\mathcal{F}_0 = 26$ MeV$^{-1}\hbar^2$ and $\mathcal{F}_1 = 121$ MeV$^{-3}\hbar^4$ have been used for all bands.

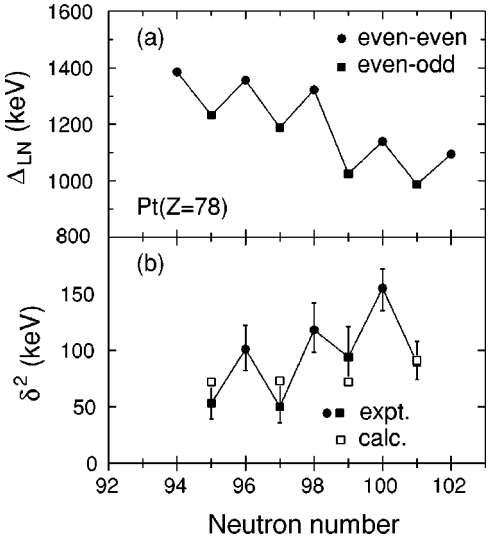

FIG. 6. (a) Calculated Lipkin-Nogami pairing gap parameter Δ_{LN} for selected even-even and odd-A Pt isotopes. (b) Experimental (filled symbols) and calculated (open symbols) α-decay reduced widths for several Pt isotopes. The calculated δ^2 values were deduced from the predicted F_α values and the experimental data for the reduced widths of the even-even neighboring nuclei (see the text for details).

can be seen from Table III, the $\nu^2(5/2^-[512], 7/2^+[633])_{K=1^-}$ configuration is predicted to be lowest in excitation energy and, therefore, appears to be the most likely candidate. Alternatively, the two-quasiparticle band could be associated with a pair of $1/2^-[541]\,(h_{9/2})$ and $1/2^+[660]\,(i_{13/2})$ proton orbitals. In fact, this configuration has been proposed to account for the high-spin structures in ^{178}Hg [5] and ^{180}Hg [6]. However, with two protons less than in the Hg isotopes, the ^{178}Pt proton Fermi level is located well below these orbitals, and therefore, their participation in such a crossing is less likely. In addition, the π^2 configuration would also be expected to be associated with a more deformed shape due to the deformation driving effects of the proton $h_{9/2}$ and $i_{13/2}$ intruder orbitals. Thus, while the π^2 structure cannot be ruled out, the ν^2 assignment is preferred. Measurements of the in-band transitional quadrupole moment would clearly help to explore the issue further.

B. The influence of pairing on the α-decay reduced width

An important observable in the α decay is the reduced width δ^2 which is defined as the ratio of the α-decay transition probability to the potential barrier penetration factor. Table V and Fig. 6(b) show the δ^2 values deduced for several deformed Pt nuclei using the formalism of Rasmussen [48]. The corresponding hindrance factors, F_α, [49] for the odd-A isotopes are also tabulated. The quoted errors were determined by taking 1σ limits on the measured α-decay energies, branching ratios and half-lives. It should be noted that Table V presents results only for nuclei where several measurements exist so that the systematic errors are greatly reduced.

The δ^2 values for the odd-A Pt isotopes are found to be approximately a factor of 2 smaller than those of the even-even neighbors. Although a similar behavior has also been noted in Ref. [50], a detailed explanation for this feature was not given. Such a trend is attributed here to differences in the pairing correlations between the even-even and odd-A isotopes. In general, the occupation of a given single-particle level near the Fermi surface in the odd isotope leads to a

TABLE V. Energies, intensities, decay branches, half-lives, reduced widths and hindrance factors for deformed Platinum α emitters.

Nucleus	E_α (keV)	I_α (%)	b_α (%)	$T_{1/2,\alpha}$ (s)	Ref.	δ^2 (keV)	F_α Expt.	Calc.
^{173}Pt	6225(9)	100	83(14)	0.376(11)	[46]	53^{+16}_{-14}	$1.9^{+0.7}_{-0.6}$	1.4
^{174}Pt	6042(5)	98.2(18)	75(8)	0.89(2)	[22]	101^{+21}_{-19}		
^{175}Pt	5960(3)	85(8)	56(5)	2.4(3)	[46,47]	50^{+20}_{-14}	$2.2^{+1.1}_{-0.8}$	1.5
^{176}Pt	5753(3)	99.74(13)	40(3)	6.3(5)	[22]	118^{+24}_{-20}		
^{177}Pt	5517(4)	88.5(7)	5.6(4)	11(1)	[47]	94^{+27}_{-18}	$1.5^{+0.6}_{-0.4}$	1.9
^{178}Pt	5447(4)	96.5(29)	7.46(28)[a]	20(1)	present	155^{+17}_{-20}		
^{179}Pt	5194(10)	100	0.24(3)	21.2(4)	[47]	89^{+19}_{-15}	1.7(4)	1.7

[a]Weighted average of the values given in Refs. [29,30].

reduction of the superfluidity, which is usually referred to as a blocking effect. It has been shown by Soloviev [49] that the stronger pairing in the even-even isotopes leads to a larger probability for the formation of an α particle inside the nucleus, since many levels near the Fermi surface participate in such a process. These predictions were supported by the observations of $F_\alpha \sim 1.2-3.0$ for favored α decays in deformed odd-A nuclei in the $A=230-250$ region [49]. In order to quantify the effect of reduced pairing for the odd-mass Pt isotopes, blocking calculations were performed using the expression given in Ref. [49]:

$$F_\alpha(a_1)=\frac{1}{2}\frac{\left[\sum_i \xi_i(N)\right]^2+\left[\sum_i \xi_i(N+2)\right]^2}{\left[\sum_{i\neq a_1} \xi_i(N+1,a_1)\right]^2}, \qquad (2)$$

where

$$\xi_i(N)=u_i(N-2)v_i(N)\prod_{j\neq i}\left[u_j(N-2)u_j(N)+v_j(N-2)v_j(N)\right], \qquad (3)$$

and u_i and v_i are the occupation coefficients, and a_1 is the blocked level. In the calculation procedure, the single-particle energies were derived from the Nilsson model with deformation parameters taken from Ref. [35]. The pairing correlations were treated using the Lipkin-Nogami prescription, and included the effect of blocking, as discussed in Sec. IV A 1. The u_i and v_i coefficients were renormalized according to the expression given in Refs. [51,52]. The calculated neutron Lipkin-Nogami pairing gaps $\Delta_{\rm LN}=\Delta+\lambda_2$, where Δ is the self-consistently determined pairing gap and λ_2 is an additional Lagrange multiplier, are shown for comparison in Fig. 6(a). Calculations predict about 10% differences in the neutron gap between the even-even and odd-even isotopes. The decrease of $\Delta_{\rm LN}$ with neutron number can be attributed to the $G\sim 1/A$ dependence of the pairing strength and the presence of a $N=98$ subshell gap at $\beta_2\sim 0.25$ which affects the density of single-particle levels near the Fermi surface. The results for the hindrance factors are presented in the last column of Table V and in Fig. 6(b). As can be seen, the calculated values show a satisfactory agreement with the experimental data. Importantly, they confirm the substantial decrease of the α-decay reduced width in the odd-A isotopes, due to the effect of blocking. It is also worth noting that the experimental δ^2 values for the even-even and the odd-A isotopes vary from nucleus to nucleus. This is an indication that other factors, such as deformation and/or configuration changes, for example, play an important role in the α-decay process. Since the neutron-deficient Pt and Os isotopes also lie at the boundaries of a region where changes towards spherical (or slightly oblate) shapes are predicted [35], one might expect that the effect of blocking on the α decay reduced widths would be less pronounced for the lighter masses because of the reduction in the density of single-particle states near the Fermi surface.

V. SUMMARY AND CONCLUSIONS

An extended level scheme for ^{178}Pt was obtained by combining the selectivity of the FMA with the high detection efficiency and resolving power of the Gammasphere γ-ray spectrometer. The ground state band was observed beyond the first crossing which is attributed to the alignment of a pair of $i_{13/2}$ neutrons. The previously known excited band was firmly assigned odd-spin and negative parity, and was considerably extended in spin. A new negative parity band was observed for the first time. The configurations of these structures were interpreted as octupole vibrations at low spin which are crossed at higher frequency by two-quasiparticle excitations. The latter are most likely neutron excitations. The large reduction of the α-decay reduced width for the odd-mass Pt isotopes is explained through the weakening of neutron pairing due to the blocking effect. Such a behavior is reproduced by blocked Nilsson-Lipkin-Nogami calculations. More precise data on α-decay energies, half-lives and branching ratios are required, however, in order to investigate this trend in detail in the more neutron deficient Pt isotopes. A study of neighboring odd-Z nuclei would also be particularly interesting as it may elucidate the role played by the proton pairing on the α-decay reduced widths.

ACKNOWLEDGMENTS

The authors wish to thank the staff of the ATLAS accelerator facility and the Physics Support Group for their assistance in various phases of the experiment. We are grateful to J. P. Greene for help with the targets. The software support by D. C. Radford and H. Q. Jin is greatly appreciated. Discussions with M. A. Riley, G. D. Dracoulis, I. Ahmad, and P. J. Woods are gratefully acknowledged. One of us (S.S.) acknowledges support from a NATO grant through the Research Council of Norway. This work is supported by the U.S. Department of Energy, Nuclear Physics Division, under Contracts No. W-31-109-ENG-38 and DE-FG02-96ER40983.

[1] J. L. Wood, K. Heyde, W. Nazarewicz, M. Huyse, and P. Van Duppen, Phys. Rep. **215**, 103 (1992).
[2] K. Heyde, P. Van Isacker, M. Waroquier, J. L. Wood, and R. A. Meyer, Phys. Rep. **102**, 293 (1983).
[3] W. C. Ma *et al.*, Phys. Rev. C **47**, R5 (1993).
[4] R. V. F. Janssens and T. L. Khoo, Annu. Rev. Nucl. Sci. **41**, 321 (1991).
[5] F. G. Kondev *et al.*, Phys. Rev. C **61**, 011303(R) (2000).
[6] F. G. Kondev *et al.* (unpublished).
[7] W. Nazarewicz, Phys. Lett. B **305**, 195 (1993).
[8] G. D. Dracoulis, J. Phys. (Paris) [Suppl.] **10**, c10 (1980).
[9] G. D. Dracoulis, C. Fahlander, and M. P. Fewell, Nucl. Phys.

A383, 119 (1982).
[10] R. M. Lieder *et al.*, Nucl. Phys. **A645**, 465 (1999).
[11] C. Fahlander and G. D. Dracoulis, Nucl. Phys. **A375**, 263 (1982).
[12] B. Cederwall *et al.*, Z. Phys. A **337**, 283 (1990).
[13] F. Soramel *et al.*, Eur. Phys. J. A **4**, 17 (1999).
[14] M. J. A. de Voigt, R. Kaczarowski, H. J. Riezebos, R. F. Noorman, J. C. Bacelar, M. A. Deleplanque, R. M. Diamond, F. S. Stephens, J. Sauvage, and B. Roussiére, Nucl. Phys. **A507**, 472 (1990).
[15] D. G. Popescu *et al.*, Phys. Rev. C **55**, 1175 (1997).
[16] K. S. Bindra *et al.*, Phys. Rev. C **51**, 401 (1995).
[17] E. S. Paul *et al.*, Phys. Rev. C **51**, 78 (1995); R. S. Simon *et al.*, Z. Phys. A **325**, 197 (1986).
[18] M. P. Carpenter *et al.*, Phys. Rev. Lett. **78**, 3650 (1997).
[19] I. Y. Lee, Nucl. Phys. **A520**, 641c (1990).
[20] C. N. Davids, B. B. Back, K. Bindra, D. J. Henderson, W. Kutschera, T. Lauritsen, Y. Nagame, P. Sugathan, A. V. Ramayya, and W. B. Walters, Nucl. Instrum. Methods Phys. Res. B **70**, 358 (1992).
[21] D. C. Radford, Nucl. Instrum. Methods Phys. Res. A **361**, 297 (1995).
[22] Y. A. Akovali, Nucl. Data Sheets **84**, 1 (1998).
[23] G. D. Dracoulis, A. E. Stuchbery, A. P. Byrne, A. R. Poletti, S. J. Poletti, J. Gerl, and R. A. Bark, Nucl. Phys. **A510**, 533 (1990).
[24] W. R. Leo, *Techniques for Nuclear and Particle Physics Experiments: A How-to Approach* (Springer-Verlag, Berlin, 1987), p. 105.
[25] E. Hagberg, P. G. Hansen, P. Hornshøj, B. Jonson, S. Mattsson, and P. Tidemand-Petersson, Nucl. Phys. **A318**, 29 (1979).
[26] J. Wauters, P. Dendooven, M. Huyse, G. Reusen, P. Van Duppen, R. Kirchner, O. Klepper, and E. Roeckl, Z. Phys. A **345**, 21 (1993).
[27] P. M. Davidson, G. D. Dracoulis, T. Kibédi, A. P. Byrne, S. S. Anderssen, A. M. Baxter, B. Fabricius, G. J. Lane, and A. E. Stuchbery, Nucl. Phys. **A657**, 219 (1999).
[28] G. D. Dracoulis, A. E. Stuchbery, A. P. Byrne, A. R. Poletti, S. J. Poletti, J. Gerl, and R. A. Bark, J. Phys. G **12**, L97 (1986).
[29] U. J. Schrewe *et al.*, Phys. Lett. **91B**, 46 (1980).
[30] P. G. Hansen, H. L. Nilsen, K. Wilsky, M. Alpsten, M. Finger, A. Lindahl, R. A. Naumann, and O. B. Nielsen, Nucl. Phys. **A148**, 249 (1970).
[31] R. S. Hager and E. C. Seltzer, Nucl. Data Sheets A **4**, 1 (1968).
[32] E. Der Mateosian and A. W. Sunyar, At. Data Nucl. Data Tables **13**, 407 (1974).
[33] K. Neergard and P. Vogel, Nucl. Phys. **A145**, 33 (1970).
[34] F. G. Kondev, G. D. Dracoulis, A. P. Byrne, T. Kibédi, and S. Bayer, Nucl. Phys. **A617**, 91 (1997).
[35] P. Möller, J. R. Nix, W. D. Myers, and W. J. Swiatecki, At. Data Nucl. Data Tables **59**, 185 (1995).
[36] R. Bengtsson and I. Ragnarsson, Nucl. Phys. **A436**, 14 (1985).
[37] W. Nazarewicz, M. A. Riley, and J. D. Garrett, Nucl. Phys. **A512**, 61 (1990).
[38] H.-Q. Jin *et al.*, Phys. Rev. C **53**, 2106 (1996).
[39] C. J. Gallagher and S. A. Moszkowski, Phys. Rev. **111**, 1282 (1958).
[40] F. G. Kondev, G. D. Dracoulis, A. P. Byrne, and T. Kibédi, Nucl. Phys. **A632**, 473 (1998).
[41] P. A. Butler and W. Nazarewicz, Rev. Mod. Phys. **68**, 349 (1996).
[42] A. Bohr and B. R. Mottelson, *Nuclear Structure* (Benjamin, Massachusetts, 1975), Vol. II, p. 191.
[43] K. E. G. Löbner, in *The Electromagnetic Interaction in Nuclear Spectroscopy* (North-Holland, Amsterdam, 1975), p. 141.
[44] R. Wyss, W. Statula, W. Nazarewicz, and A. Johnson, Nucl. Phys. **A511**, 324 (1990).
[45] P. Vogel, Phys. Lett. **60B**, 431 (1976).
[46] R. D. Page, P. J. Woods, R. A. Cunningham, T. Davinson, N. J. Davis, A. N. James, K. Livingston, P. J. Sellin, and A. C. Shotter, Phys. Rev. C **53**, 660 (1996).
[47] *Table of Isotopes*, edited by R. B. Firestone (Wiley, New York, 1996).
[48] J. O. Rasmussen, Phys. Rev. **113**, 1593 (1959).
[49] V. G. Soloviev, *Theory of Complex Nuclei* (Pergamon Press, Oxford, 1976), p. 191.
[50] C. R. Bingham *et al.*, Phys. Rev. C **54**, R20 (1996).
[51] L. Bennour, P-H. Heenen, P. Bonche, J. Dobaczewski, and H. Flocard, Phys. Rev. C **40**, 2834 (1989).
[52] P. Quentin, N. Redon, J. Meyer, and M. Meyer, Phys. Rev. C **41**, 341 (1990).